# Large Temperature Dependent Spin Orbit Coupling in Electron-Electron Interaction Dominated Orthorhombic $SrIrO_3$ Film

Lunyong Zhang,[1] Y. B. Chen*,[2] Jian Zhou,[1] Shan-Tao Zhang,[1] Zheng-bin Gu,[1] Shu-Hua Yao,[1] and Yan-Feng Chen[1]

[1] National Laboratory of Solid State Microstructures & Department of Materials Science and Engineering, Nanjing University, Nanjing 210093 China

[2] National Laboratory of Solid State Microstructures & Department of Physics, Nanjing University, Nanjing 210093 China

* Corresponding author Y.B Chen E-mail: ybchen@nju.edu.cn

ABSTRACT: The spin orbit coupling in orthorhombic $SrIrO_3$ film was studied at different temperatures via weak anti-localization effect. The spin orbit coupling increased with the increasing temperature in the regime of two dimensional variable range hopping conduction. Near linearly temperature dependent Rashba coefficient was manifested and interpreted through the electron correlation assisted evolution of Landé *g* factor, which was assumed to be linearly decrease with temperature rising. Moreover, the $t_{2g}$ band of orthorhombic $SrIrO_3$ is not fully separated into $J_{eff}$=1/2 and $J_{eff}$=3/2 bands, as proved by the Landé *g* factor at zero temperature with a value of 1.0568 which is between that corresponding to non-splitted $t_{2g}$ band and that to fully splitted $t_{2g}$ band.

KEYWORDS: Spin orbit coupling, $SrIrO_3$ film, Rashba coefficient, Temperature dependence, Landé *g* factor.

## INTRODUCTION

Spin orbit coupling (SOC) is a relativistic effect originating from 'the electromagnetic interaction between the electron's spin and the magnetic field generated by the electron's orbit around the nucleus'[1]. It has attracted much attention since it can not only induce spin relaxation, a central topic of the recently developed *spintronics* with expectation to conquer the fatal problems prohibiting the further development of modern electronic technologies through manipulating the spin degree of charge carrier[2], but also trigger a large number of novel physical phenomena such as topological insulator [3] and quantum phase transitions[4].

The works on SOC so far have been largely carried out in III-V and II-VI semiconductors with weak electron correlation. It is indicated that SOC can be introduced into actual materials by the

structure inversion asymmetry (Rashba effect) as well as the bulk inversion asymmetry (Dresselhaus effect) [5], and can be modulated by several methods. For example, strain can induce and enhance different SOC type combinations in semiconductor system and trigger various behaviors of electron spin manipulation [6]. The Rashba SOC is significantly affected by electric field so bears great convenience for device applications [7]. Here we studied the temperature dependence of SOC in a typical metallic oxide, $SrIrO_3$ (SIO). It is strictly substantial for device design and application and has been recently noticed showing unpredicted behaviors in a few of semiconductors.

Compared with semiconductors, the transition metal oxides always indicate diversely nontrivial physical behaviors such as high temperature superconductivity, charge and spin density wave, giant magnetoresistance and quantum phase transition as the results of complex interactions among charge, spin, orbit and crystal field [10, 11]. $SrIrO_3$ is a typical metallic oxide with strong SOC (≈0.3-0.4ev) and electron correlation(≈0.5ev) simultaneously [8]. Its homolog $Sr_2IrO_4$ is famous as a SOC assistant Mott insulator[9]. It is interesting and reasonable to suppose the temperature effect of SOC in $SrIrO_3$ may be different from that in semiconductors. Several works have stated the electron-electron interaction enhanced spin-orbit splitting which would modify electronic structure dramatically [12-14].

Considering the temperature dependence of SOC, the experimental results on CuBr[15], $In_{0.86}Ga_{0.14}As_{0.83}Sb_{0.17}$ epilayer [16] showed a temperature independent spin orbit splitting. Contrarily, the Rashba coefficient was found to linearly increase with temperature in a wide temperature range for a (110)-oriented GaAs/AlGaAs quantum well [17] and a symmetric Te doping n-InSb/InAlSb quantum well[18]. However in a asymmetric Te doping n-InSb/InAlSb quantum well the Rashba coefficient linearly increases at the beginning and then linearly decreases with temperature raise [18]. Interestingly, these experimental results indicating temperature dependent Rashba SOC are not in consistent with the $k \cdot p$ theory which predicts temperature independent Rashba coefficient[17]. *Eldridge et al.* have attributed this to the usually neglected higher-order terms in the Rashba Hamiltonian in the enlightenment of the kinetic energy dependent of Zeeman splitting[17]. Nevertheless, a fully and explicitly theoretical explanation is still missing.

In the present work, we adopted the anti-localization related magnetoconductance fitting method to study the SOC of $SrIrO_3$ films. A similarly near linear temperature dependence of Rashba coefficient was observed, which was further interpreted based on the Landé $g$ factor variation with

temperature.

## EXPERIMENTAL

The SIO films were synthesized on (001)-$SrTiO_3$ (STO) substrates by pulsed laser deposition (PLD) with a Brilliant Nd:YAG Laser of 355 nm laser and 160 mJ pulse energy at 750℃ substrate temperature and 10/3 Hz laser pulse frequency in 25Pa oxygen atmosphere. The film growth duration was 10min. Detailed synthesis process can be browsed in Ref [19]. The substrates were supplied by the Shanghai Daheng Optics and Fine Mechanics Co. Ltd. The miscut angle is less than 0.5°. Before films synthesis, the STO substrates were soaked in 70℃ deionized water for 10min, successively were ultrasonic washed by acetone and deionized water, respectively for 5min. After that the substrates were etched in 10mol/L $NH_4F$ solution buffering HF (PH=4.5) for 40s, then they were annealed at 1000 ℃ in oxygen flow for 2.5h to remove the distorted layer due to polishing [20].

The x-ray diffraction (XRD) was carried out by a 2.4kW Rigaku Rota flex X-ray diffractometer with Cu-kα ray. The film surface morphologies were recorded by an Asylum cypher atomic formce microscopy (AFM). The film thicknesses *d* were calibrated to be about 7nm through a Tecnai F20 transmission electron microscopy (TEM). Electron transport measurements were carried out on a physical property measurement system (PPMS, Quantum Design) through the four-probe method.

## RESULTS AND DISSCUSSIONS

The AFM image (Fig.1 inset) shows a typical smooth surface morphology with two dimensional growth model for the sample $SrIrO_3$ film. Its XRD pattern (Fig.1) further indicates a matrix with orthorhombic phase which is consistent with our previous systematic research on the microstructure of $SrIrO_3$ films on (001)-$SrTiO_3$ substrates through TEM [19] and the reports of Kim [21].

The sample film shows obvious metal insulator transition with transition temperature about 28K (Fig.2a), indicating that quantum conductivity correction effects have emerged. In general, weak localization and electron-electron interaction could be ascribed to the quantum conductivity correction mechanisms and they can be considered together through a temperature dependent resistivity model [22]

$$\rho(T) = \frac{1}{\sigma_0 + a_1 T^{p/2} + a_2 T^{1/2}} + bT^q \qquad (1)$$

where $\sigma_0$ labels the classical temperature-independent Drude conductivity, $a_1$ and $a_2$ respectively

account for the weak localization contribution and the electron-electron interaction mechanism. $p$ describes localization effects, $p$=2 implies the dominance of electron-electron interaction and electron-phonon scattering is the dominator if $p$=3[22]. The term $bT^q$ comes from normal inelastic scatterings, for example the electron phonon scattering; $q$ depends on the scattering mechanism. Further by noting the relation $\rho$=$Rd$ of the four probe method, we found the temperature dependent resistance shown in Fig.2a can be soundly fitted in the temperature range above 10K by Eq.1 with $p$≈3, $q$≈0.44, $\sigma_0$≈647.58Ohm$^{-1}$cm$^{-1}$, $a_1$≈26.03Ohm$^{-1}$cm$^{-1}$K$^{-1}$, $a_2$≈98.89Ohm$^{-1}$cm$^{-1}$K$^{-1/2}$ and $b$≈1.16×10$^{-5}$ Ohm cm K$^{-q}$. Therefore, weak localization is responsible for the metal insulator transition. It is further confirmed by the magnetoconductance patterns shown in Fig.3. Moreover, electron-electron interaction takes a great impact on the sample conduction, in accordance with the strongly correlated feature of $SrIrO_3$ and the electron carrier conclusion drawn from the standard Hall effect detection (representatively shown as inset of Fig.5). Latter we will see again the electron-electron interaction is the dominating mechanism responsible for the inelastic scattering.

To clarify the conduction mechanism below 10K, the typical variable range hopping process in weak localization regime is considered based on the method proposed by *Hill*, et al. [23, 24]. As briefly shown in Fig.2b, variable range hopping related conduction behavior is obvious. The hopping dimensional indexed by $D$ accurately equals two, implying that the film can be considered as a two dimensional electronic system [25] and is a great suitable platform for SOC study.

According to the well founded quantum correction theory of magnetoconductance, a system simultaneously exhibiting SOC and weak localization should have a concave shape conductance curve under a varied external magnetic field[26]. Fig.3 illustrates the magneto-conductance traces at several temperatures of the $SrIrO_3$ film sample. All of them show characteristic concave shape at temperatures above 2K. The decrease of magneto-conductance in low field is caused by the SOC inducing weak anti-localization effect. After the conductance minimum, the weak anti-localization effect causing conductance decrease is no longer larger than the conductance increase originated from the weak localization breakdown under magnetic field. The field corresponding to the conductance minimum, $B_{min}$, is believed to approximately proportionate to the SOC strength[27], therefore a rough conclusion can be drawn that the SOC strength of the $SrIrO_3$ film in the investigated temperature range exhibits a positive correlation to temperature.

In theory, magnetoconductance with quantum correction in low field around $B_{min}$ could be formulated by the Hikami-Larkin-Nagaoka equation[26]

$$\frac{\Delta G}{G_u}=\psi\left(\frac{1}{2}+\frac{B_e}{B}\right)-\psi\left(\frac{1}{2}+\frac{B_i+B_{soc}}{B}\right)+\frac{1}{2}\left[\psi\left(\frac{1}{2}+\frac{B_i}{B}\right)-\psi\left(\frac{1}{2}+\frac{B_i+2B_{soc}}{B}\right)\right] \quad (2)$$

where $\psi(x)$ is the digamma function, $\Delta G=G(B)-G(B=0)$ and $G_u=e^2/(\pi h)\approx 1.2\times10^{-5}$S is a universal value of conductance. The $B_e$, $B_i$ and $B_{soc}$ are the equivalent fields of elastic scattering, inelastic scattering and the scattering induced by SOC, respectively. Their magnitudes mean the corresponding scattering strengths. All of them can be expressed as functions of their scattering lengths $l_o$ (o=e, i and soc), $B_o=\hbar/4el_o^2$ [28]. Fig.4a and Fig.4b give out the fitted $B_i$ and $B_{soc}$ at different temperatures. Here the fitted $B_e$ are not shown since large uncertainties on $B_e$ are tolerant for soundly fitting the magnetoconductance curves. By contrast, even a small variation of the $B_i$ or $B_{soc}$ ($\delta B_i<10\%$ and $\delta B_{soc}<5\%$) would cause obvious deviation in the fitting. Whatever, the magnitude of $B_e$ is at a order 1~10T, strictly larger than $B_i$ and $B_{soc}$. This suggests an elastic scattering length of 10~40nm, which is quite short comparing to the micron scaled elastic scattering length of typical semiconductor wells [27, 29] and approximate to the sample thickness. The $B_i$ is around 0.03T, leading an inelastic scattering length $l_i$ at a scale of ~200nm. It is close to those of ultrathin bismuth film [30] and graphene [31] at mesoscopic scale. Given that a mesoscopic system is defined by the sample size dimension lower than the inelastic scattering length, our $SrIrO_3$ film has been a mesoscopic system in the growth direction since its thickness is about 7nm which is markedly smaller than its inelastic scattering length. In a mesoscopic system, all the particle collisions would be mainly dominated by elastic scattering, the coherent backscattering and the interference of particles are enhanced [32]. This explains the strongly elastic scattering and the two dimensional hopping conduction features in the sample (Fig.2b).

Moreover, the $B_i$ seemly is not temperature sensitive in the measuring temperature range (Fig.4a), suggesting a non-temperature dependent inelastic scattering length. This is rare in normal system like metals where inelastic scattering length conventionally bears $T^{-v}$ relation with temperature. According to the wave scattering theory, a temperature dependent inelastic scattering length is held for quantum wave which means diffusion transport for a electron system, and the inelastic scattering length is generally insensitive to temperature for a classic wave case such as the electron transport in weak localization state [32]. Actually, a non-temperature dependent inelastic scattering length also has been observed in a epitaxial graphene showing weak localization behavior[31]. Consequently, it is reasonable that the sample here demonstrates a temperature insensitive inelastic scattering length. If the relation $l_i=\sqrt{D\tau_i}$ is adopted ($D$ is carrier diffusion coefficient and can be related to carrier mobility $\mu$ by the Einstein model $D=\mu k_B T e^{-1}$, $\tau_i$ represents

the inelastic scattering relaxation time), we can derived that $\tau_i$ is approximately proportional to $T^{-1}$ on the basis of the carrier mobility temperature dependence obtained from the standard Hall effect measurement (Fig.5). Therefore, we proved again that the SIO film sample is a two dimensional system with strong electron-electron interaction impacting on its electron transport since $\tau_i \propto T^{-1}$ corresponds to a carrier-carrier scattering dominated two dimensional system[33].

As for the SOC equivalent filed $B_{soc}$ (Fig.4b), it is at a order of 0.1T, noticeably larger than those of many typical semiconductors (1μT-10mT)[27, 34]. More important is that $B_{soc}$ follows an excellent $T^2$ dependent relation. It leads a near linearly temperature dependent Rashba SOC coefficient $\alpha$ (Fig.4c) based on the expression $\alpha=m_*^{-1}\left(e\hbar^3 B_{soc}\right)^{1/2}$ [28] (our previous work showed a Rashba type SOC in orthorhombic $SrIrO_3$ film [35]). This is not anticipated by traditional views but same as the recent discovering in a few of semiconductor quantum wells [17, 18]. Here $m_*$ refers the effective electron mass, it equals to $7m_0$ for $SrIrO_3$[36] ($m_0$ is the free electron mass). Actually if we neglect the band structure effect on the SOC, which is reasonable since the band gap of orthorhombic $SrIrO_3$ is about 100meV[8], the Rashba coefficient could be expressed as a function of Landé $g$ factor, asymmetric structure induced electric field $\varepsilon$, light speed $c$ and electron effective mass [2]

$$\alpha = g\left(g-1\right)\frac{\pi e\hbar^2\varepsilon}{4m_*^2c^2} \tag{3}$$

Many experiments have proved in fact that the Landé $g$ factor can be influenced by temperature, and in most cases shows near linear temperature dependence[37, 38]. Therefore, we have a modified Rashba coefficient expression by substituting $g=g_0+\lambda T$ into Eq.3 that is

$$\alpha = \left[g_0\left(g_0-1\right)+\left(2g_0-1\right)\lambda T+\lambda^2T^2\right]\frac{\pi e\hbar^2\varepsilon}{4m_*^2c^2} \tag{4}$$

Using Eq.4 the Rashba coefficient shown in Fig.4c could be soundly fitted with $g_0$=1.0568, $\lambda$=-0.033 and $\varepsilon \approx 5.15\times10^{14}$ V/m (greatly smaller than that of typical semiconductor systems, ~$10^{25}$ V/m [18]). Ref [9] has been stated that the regular $t_{2g}$ band with orbital angular momentum $L$=1 and spin angular momentum $S$=1/2 for $5d^5$-$Ir^{4+}$ would be splitted into effective total angular momentum $J_{eff}$=1/2 doublet with high energy and $J_{eff}$=3/2 quartet bands with low energy in the strong SOC limiting. Thus, the Landé $g$ factor could be calculated to be about 0.7 in the strong SOC limiting with $S$=1/2, $L$=1 and $J$=1/2 through the Landé $g$ factor

expression $g = 1.5 + \left[S(S+1) - L(L+1)\right] / 2J(J+1)$. In the weak SOC limiting (without SOC splitting), the Landé *g* factor is 1.3 calculated with $S$=1/2, $L$=1 and $J$=$L$+$S$=3/2. It is obvious that the $g_0$ above for well fitting the Rashba SOC coefficient data is between them, implying the $t_{2g}$ band would be not fully splitted into separated $J_{eff}$=1/2 and $J_{eff}$=3/2 bands by SOC in metallic orthorhombic $SrIrO_3$ and the bandwidths of the mixed band would be larger than that corresponding to fully splitted bands for example the separated $J_{eff}$=1/2 and $J_{eff}$=3/2 bands in Mott insulator $Sr_2IrO_4$. This reconfirms that the SOC is critical for the determination of band structure and electron transport feature in 5d iridium oxides. It also manifests that the fitting of $\alpha$ with Eq.4 is appropriate.

Regarding to the temperature dependence of Landé *g* factor, many works have been done in the past decades in typical semiconductor systems like the GaAs and InSb because the measured *g* factor is always discrepant on the prediction by *k.p* theory. An accepted viewpoint on the discrepancy is based on the fact that the band gap would shrink with the temperature increase inducing lattice expansion, which would cause a decreasing *g* factor. *Litvinenko et.al* has stated that the observed *g* factor temperature dependence in both InSb and GaAs could be explained in the frame of *k.p* theory by only taking the dilational variation of energy gap into account [39]. We therefore believe that the band gap shrinkage mechanism above is basically applicable to our $SrIrO_3$ system. Moreover, we noted that the fitting slop of the *g* factor variation on temperature is strictly larger than that of the typical semiconductor systems about 1-2 order in magnitude, suggesting another factor impacting on band gap may exist besides the lattice expansion. It has been manifested before that electron-electron interaction is the main dominator of our sample transport properties. This is a natural result of the strongly correlated feature of $SrIrO_3$. According to the founded knowledge of 5d Iridium compounds, electron correlation energy $U$ is a critical interaction except of the SOC who configure the special band structures, which is quite different from the circumstance of traditional semiconductor systems. Otherwise, Ref. 40 has proved that electron correlation energy could be depressed by increased temperature. Accordingly, we propose here a large shrinkage of band gap would be induced by the electron correlation energy decrease when temperature is enhanced, which together with the lattice expansion induced band gap shrinkage creates the large slop of the *g* factor variation on temperature. In fact, it is well recognized that the effective mass is also affected by temperature, so similarly would has attribution to the Rashba coefficient variation on temperature. However, this effect could be neglected comparing to the *g* factor attribution since the temperature dependence of the effective mass is generally much weaker than that of the *g* factor [40].

## CONCLUSIONS

In summary we observed that the spin orbit coupling elevates with the increase of temperature under a parabolic dependent relation, leading to a near linearly temperature dependent Rashba spin orbit coupling coefficient which can be soundly explained by assuming the Landé *g* factor to be linear decreasing with temperature enhancement. This explanation is also suitable for the semiconductor systems like the GaAs/AlGaAs quantum wells and InSb/InAlSb quantum wells in which similar near linearly temperature dependent Rashba coefficients have been detected. Detail analyses demonstrated that electron electron scattering is the dominating scattering mechanism in the electron transport of orthorhombic $SrIrO_3$ film no matter in the low temperature range corresponding to two dimensional variable range hopping conduction or at higher temperature range. This strongly electron correlation is proposed as the major attributor causing the rapid drop of the *g* factor with temperature rising.


## ACKNOWLEDGEMENTS

We'd like to acknowledge the financial support from the Nation Science Foundation of China (50632030 and 10974083), the New Century excellent talents in University (NCET-09-0451), the China Postdoctoral Science Foundation (2013M530250) and the Jiangsu Province Postdoctoral Science Foundation (1202001C).


## REFERENCES


1. http://en.wikipedia.org/wiki/Spin%E2%80%93orbit_interaction.
2. S. Bandyopadhyay and M. Cahay, *Introduction to spintronics*, CRC press Boca Raton, FL2008.
3. M. König, S. Wiedmann, C. Brüne, A. Roth, H. Buhmann, L. W. Molenkamp, X.-L. Qi and S.-C. Zhang, *Science*, 2007, **318**, 766-770.
4. T. Sumanta, D. S. Tudor, D. S. Jay and S. D. Sarma, *New J. Phys.*, 2011, **13**, 065004.
5. R. Winkler, *Spin-orbit coupling effects in two-dimensional electron and hole systems*, Springer Verlag2003.
6. Y. Li and Y. Q. Li, *The European Physical Journal B*, 2008, **63**, 493-500.
7. S.-M. HUANG, *Int. J. Mod. Phys. B*, 2012, **26**, 1230015.
8. S. J. Moon, H. Jin, K. W. Kim, W. S. Choi, Y. S. Lee, J. Yu, G. Cao, A. Sumi, H. Funakubo, C. Bernhard and T. W. Noh, *Physical Review Letters*, 2008, **101**, 226402.
9. B. J. Kim, H. Jin, S. J. Moon, J. Y. Kim, B. G. Park, C. S. Leem, J. Yu, T. W. Noh, C. Kim, S. J. Oh, J. H. Park, V. Durairaj, G. Cao and E. Rotenberg, *Physical Review Letters*, 2008, **101**,

076402.

10. V. Turkowski and J. Freericks, *Strongly Correlated Systems, Coherence and Entanglement*2007.
11. P. Fulde, P. Thalmeier and G. Zwicknagl, in *Solid State Physics*, eds. E. Henry and S. Frans, Academic Press2006, pp. 1-180.
12. G.-Q. Liu, V. N. Antonov, O. Jepsen and O. K. Andersen, *Physical Review Letters*, 2008, **101**, 026408.
13. S. Sarkar, M. De Raychaudhury, I. Dasgupta and T. Saha-Dasgupta, *Physical Review B*, 2009, **80**, 201101.
14. H.-S. Jin and K.-W. Lee, *Physical Review B*, 2011, **84**, 172405.
15. S. Lewonczuk, J. G. Gross and J. Ringeissen, *J. Physique Lett.*, 1981, **42**, 91-94.
16. M. Motyka, F. Janiak, G. Sek, J. Misiewicz and K. D. Moiseev, *Applied Physics Letters*, 2012, **100**, 211906-211904.
17. P. S. Eldridge, W. J. H. Leyland, P. G. Lagoudakis, O. Z. Karimov, M. Henini, D. Taylor, R. T. Phillips and R. T. Harley, *Physical Review B*, 2008, **77**, 125344.
18. M. A. Leontiadou, K. L. Litvinenko, A. M. Gilbertson, C. R. Pidgeon, W. R. Branford, L. F. Cohen, M. Fearn, T. Ashley, M. T. Emeny, B. N. Murdin and S. K. Clowes, *Journal of Physics: Condensed Matter*, 2011, **23**, 035801.
19. L. Zhang, H.-Y. Wu, J. Zhou, F.-X. Wu, Y. B. Chen, S.-H. Yao, S.-T. Zhang and Y.-F. Chen, *Applied Surface Science*, 2013, **280**, 282-286.
20. A. Biswas, P. B. Rossen, C. H. Yang, W. Siemons, M. H. Jung, I. K. Yang, R. Ramesh and Y. H. Jeong, *Applied Physics Letters*, 2011, **98**, 051904-051903.
21. Y. K. Kim, A. Sumi, K. Takahashi, S. Yokoyama, S. Ito, T. Watanabe, K. Akiyama, S. Kaneko, K. Saito and H. Funakubo, *Japanese journal of applied physics*, 2006, **45**, L36-L38.
22. E. J. Moon, B. A. Gray, M. Kareev, J. Liu, S. G. Altendorf, F. Strigari, L. H. Tjeng, J. W. Freeland and J. Chakhalian, *New J. Phys.*, 2011, **13**, 073037.
23. A. Zabrodskii and K. Zinov'eva, *Zh. Eksp. Teor. Fiz*, 1984, **86**, 742 [Sov. Phys. JETP 1984, 1959, 1425 ].
24. R. M. Hill, *physica status solidi (a)*, 1976, **35**, K29-K34.
25. M. Pollak and B. I. Shklovskii, *Hopping transport in solids*, North-Holland1990.
26. S. Hikami, A. I. Larkin and Y. Nagaoka, *Progress of Theoretical Physics*, 1980, **63**, 707-710.
27. S. Faniel, T. Matsuura, S. Mineshige, Y. Sekine and T. Koga, *Physical Review B*, 2011, **83**, 115309.

28. C. Schierholz, T. Matsuyama, U. Merkt and G. Meier, *Physical Review B*, 2004, **70**, 233311.
29. R. L. Kallaher, J. J. Heremans, N. Goel, S. J. Chung and M. B. Santos, *Physical Review B*, 2010, **81**, 075303.
30. S. Sangiao, N. Marcano, J. Fan, L. Morellón, M. R. Ibarra and J. M. D. Teresa, *EPL (Europhysics Letters)*, 2011, **95**, 37002.
31. S. Lara-Avila, A. Tzalenchuk, S. Kubatkin, R. Yakimova, T. J. B. M. Janssen, K. Cedergren, T. Bergsten and V. Fal'ko, *Physical Review Letters*, 2011, **107**, 166602.
32. P. Sheng, *Introduction to Wave Scattering: Localization and Mesoscopic Phenomena*, Springerverlag Berlin Heidelberg2006.
33. D. K. Ferry, S. M. Goodnick and J. P. Bird, *Transport in nanostructures*, Cambridge University Press2009.
34. G. L. Chen, J. Han, T. T. Huang, S. Datta and D. B. Janes, *Physical Review B*, 1993, **47**, 4084-4087.
35. F. X. Wu, J. Zhou, L. Y. Zhang, Y. B. Chen, S. T. Zhang, Z. B. Gu, S. H. Yao and Y. F. Chen, *Journal of Physics: Condensed Matter*, 2013, **25**, 125604. Actually in our opinion the SOC in $SrIrO_3$ also contains the attribution of the intrinsic SOC related to the heavy mass of iridium atom. However, to our knowledge, an effective method to distinguish the intrinsic SOC from the Rashba SOC and the Dresselhaus SOC in experiments is still absent and the Hikami-Larkin-Nagaoka model Eq.2 also takes only a gross SOC into account and does not distinguish the SOC source, the Rashba coefficient latter discussed so could be considered as an effective Rashba coefficient composed of two types SOC, the main Rashba SOC and the intrinsic SOC
36. D. N. Basov, R. D. Averitt, D. van der Marel, M. Dressel and K. Haule, *Reviews of Modern Physics*, 2011, **83**, 471-541.
37. B. K. Meyer, A. Hofstaetter, U. Leib and D. M. Hofmann, *Journal of Crystal Growth*, 1998, **184–185**, 1118-1122.
38. M. Oestreich and W. W. Rühle, *Physical Review Letters*, 1995, **74**, 2315-2318.
39. K. L. Litvinenko, L. Nikzad, C. R. Pidgeon, J. Allam, L. F. Cohen, T. Ashley, M. Emeny, W. Zawadzki and B. N. Murdin, *Physical Review B*, 2008, **77**, 033204.
40. M. W. C. Dharma-wardana, *Physical Review B*, 2005, **72**, 125339.

## FIGURE CAPTIONS

Fig.1 XRD pattern and AFM image of the sample. The squares in XRD pattern mark the faint impure peaks belonging to the monoclinic phase $SrIrO_3$.

Fig.2 Resistance-temperature curve a), RT, of the sample and b) the transformed curve of RT according to the variable range hopping model (VRH) and the related Hill-Zabrodskii-Zinov'eva VRH data treatment method shown in the figure.

Fig.3 Magnetoconductance traces of the sample under different temperature. Dots are the experimental data and solid curves are the fitting results according to Eq.2

Fig.4 Characteristic parameters of the magnetoconductance traces shown in Fig.3, a) the inelastic scattering equivalent field, b) the spin orbit coupling equivalent field and c) the derived Rashba SOC coefficient, where the dash dot curve is obtained by fitting through Eq.4 with $g$=1.0568-0.033$T$ and $\varepsilon \approx 5.15\times10^{14}$ V/m.

Fig.5 Temperature dependent traces of the electron mobility measured through standard Hall Effect detection. The inset figure shows the Hall resistance at 6K as an example. The mobility is calculated individually at the low field and the high field denoted in the inset figure because slop change in the Hall resistance pattern owing to anomalous Hall Effect appears.

Fig.1

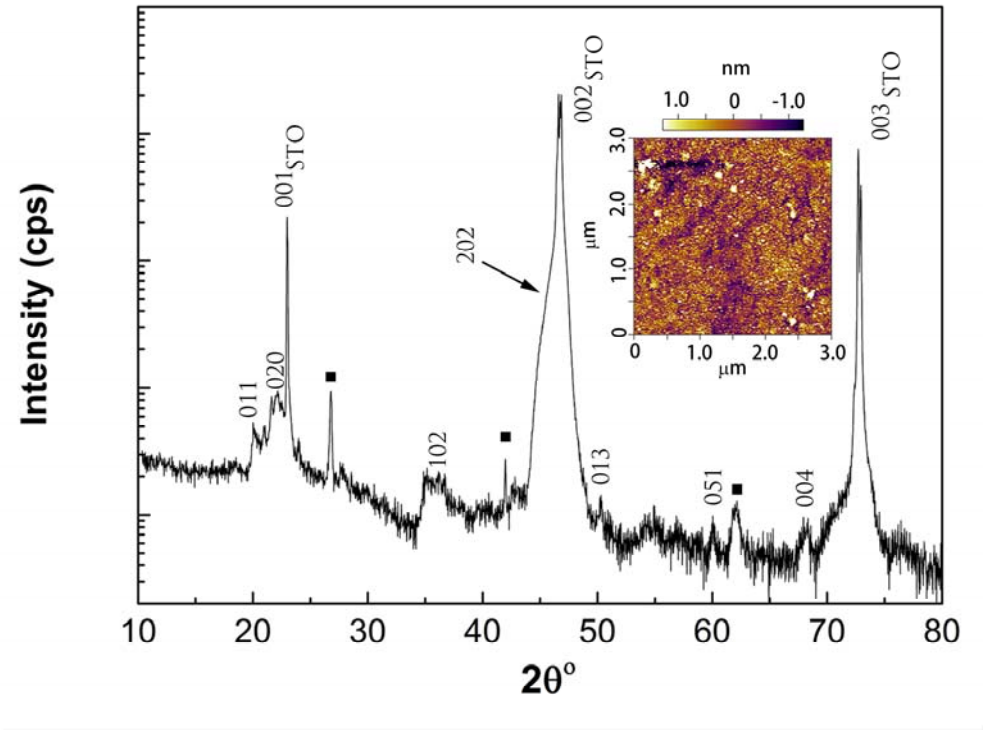
Intensity (cps)
2θ°
001STO
002STO
003STO
011
020
202
102
013
051
004
nm
1.0
0
-1.0
μm
μm

Fig.2

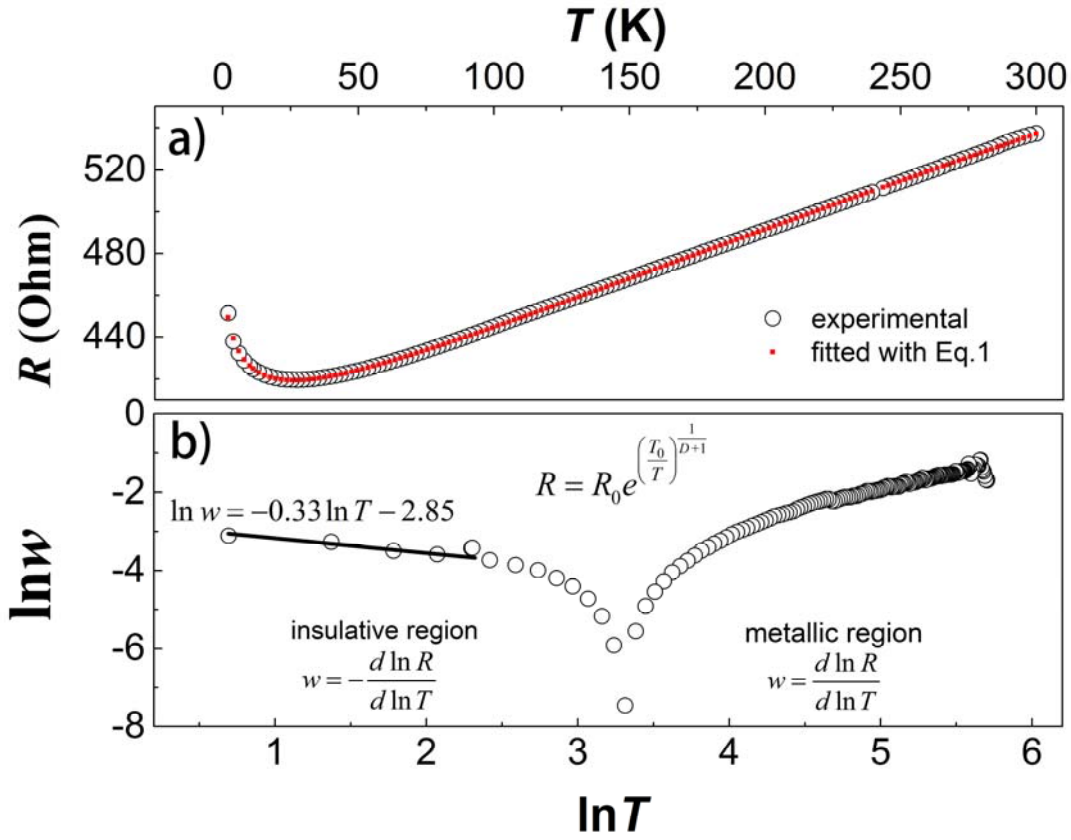
T (K)
0
50
100
150
200
250
300
a)
R (Ohm)
520
480
440
experimental
fitted with Eq.1
b)
lnw
0
-2
-4
-6
-8
$\ln w = -0.33 \ln T - 2.85$
$R = R_0 e^{\left(\frac{T_0}{T}\right)^{\frac{1}{D+1}}}$
insulative region
$w = -\frac{d \ln R}{d \ln T}$
metallic region
$w = \frac{d \ln R}{d \ln T}$
1
2
3
4
5
6
lnT

Fig.3

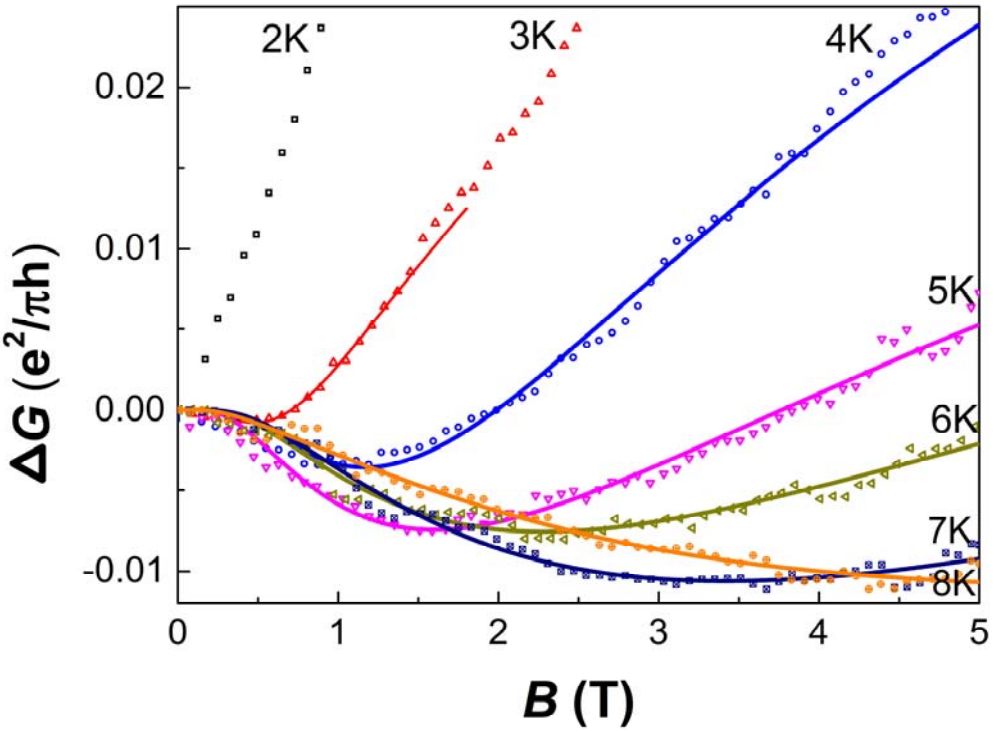

Fig.4

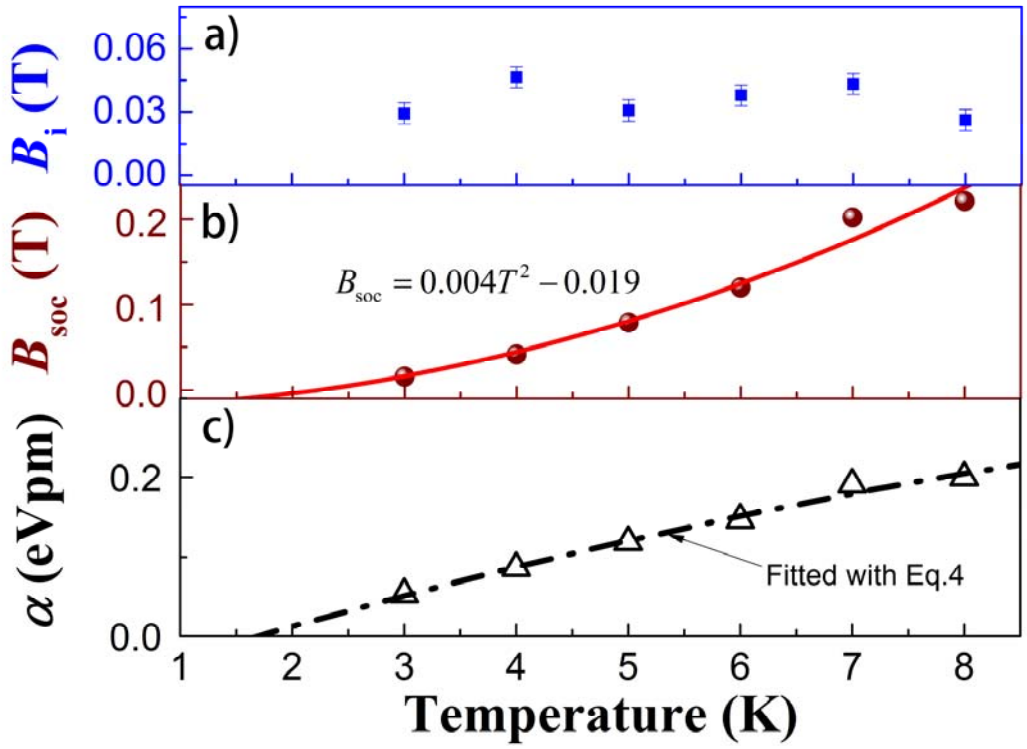
a)
b)
c)
$B_i$ (T)
$B_{soc}$ (T)
$\alpha$ (eVpm)
$B_{soc} = 0.004T^2 - 0.019$
Fitted with Eq.4
Temperature (K)
0.06
0.03
0.00
0.2
0.1
0.0
0.2
0.0
1
2
3
4
5
6
7
8

Fig.5

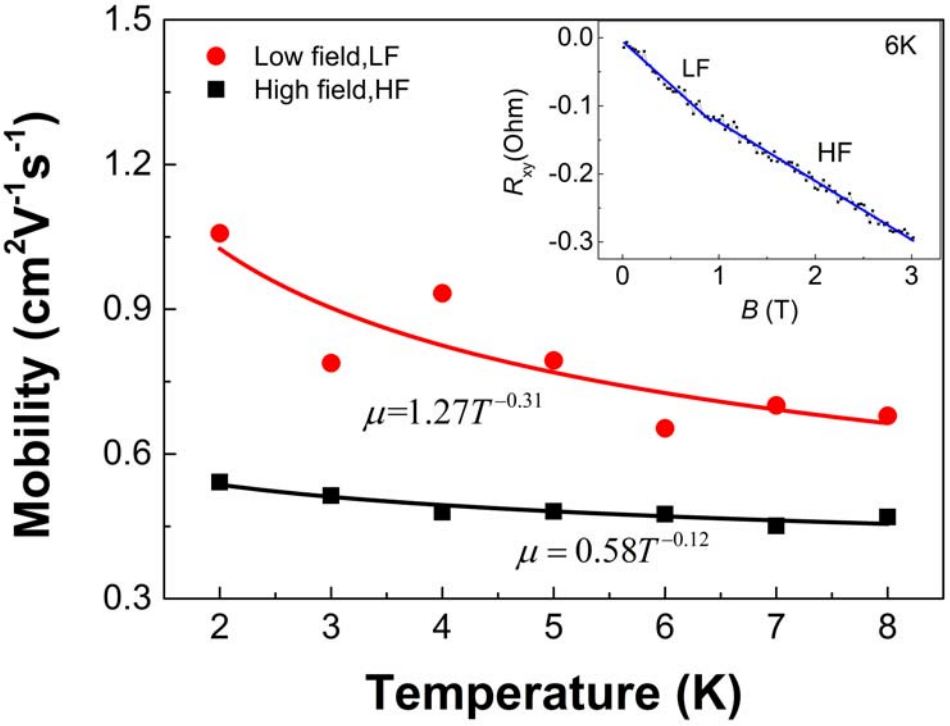
Low field,LF
High field,HF
$\mu$=1.27$T^{-0.31}$
$\mu$ = 0.58$T^{-0.12}$
Mobility ($cm^2V^{-1}s^{-1}$)
Temperature (K)
6K
LF
HF
$R_{xy}$(Ohm)
B (T)